HHS Public Access

Author manuscript

Circ Res. Author manuscript; available in PMC 2019 December 07.

Published in final edited form as:

Circ Res. 2018 December 07; 123(12): 1285–1297. doi:10.1161/CIRCRESAHA.118.313089.

Myofibroblast Specific TGFβ Receptor II Signaling in the Fibrotic Response to Cardiac Myosin Binding Protein C-Induced Cardiomyopathy

Qinghang Meng[1], **Bidur Bhandary**[1], **Md. Shenuarin Bhuiyan**[2], **Jeanne James**[3], **Hanna Osinska**[1], **Iñigo Valiente-Alandi**[1], **Kritton Shay-Winkler**[1], **James Gulick**[1], **Jeffery D. Molkentin**[1], **Burns C. Blaxall**[1], and **Jeffrey Robbins**[1]

[1]Division of Molecular Cardiovascular Biology, Cincinnati Children's Hospital, Cincinnati, Ohio;

[2]Department of Molecular and Cellular Physiology & Department of Pathology and Translational Pathobiology, Louisiana State University Health Sciences Center, Shreveport, LA;

[3]Division of Pediatric Cardiology, Medical College of Wisconsin, Milwaukee, WI

Abstract

Rationale: Hypertrophic cardiomyopathy occurs with a frequency of about 1 in 500 people. Approximately 30% of those affected carry mutations within the gene encoding cardiac myosin-binding protein C (cMyBP-C). Cardiac stress, as well as cMyBP-C mutations, can trigger production of a 40kDa truncated fragment derived from the amino terminus of cMyBP-C (Mybpc3^{40kDa}). Expression of the 40kDa fragment in mouse cardiomyocytes leads to hypertrophy, fibrosis and heart failure. Here we use genetic approaches to establish a causal role for excessive myofibroblast activation in a slow, progressive genetic cardiomyopathy - one that is driven by a cardiomyocyte-intrinsic genetic perturbation that models an important human disease.

Objective: Transforming growth factor-β (TGFβ) signaling is implicated in a variety of fibrotic processes and the goal of this study was to define the role of myofibroblast TGFβ signaling during chronic *Mybpc3^{40kDa}* expression.

Methods and Results: To specifically block TGFβ signaling only in the activated myofibroblasts in *Mybpc3^{40kDa}* transgenic (Tg) mice, quadruple compound mutant mice were generated, in which the TGFβ receptor II (TβRII) alleles (*Tgfbr2*) were ablated using the *Postn* (periostin) allele, myofibroblast-specific, tamoxifen-inducible Cre (*Postnmcm*) gene-targeted line. *Tgfbr2* was ablated either early or late during pathological fibrosis. Early myofibroblast specific *Tgfbr2* ablation during the fibrotic response reduced cardiac fibrosis, alleviated cardiac hypertrophy, preserved cardiac function, and increased lifespan of the *Mybpc3^{40kDa}* Tg mice. *Tgfbr2* ablation late in the pathological process reduced cardiac fibrosis, preserved cardiac function, and prolonged *Mybpc3^{40kDa}* mouse survival but failed to reverse cardiac hypertrophy.

Address correspondence to: Dr. Jeffrey Robbins, 240 Sabin Way, MLC7020, Cincinnati Children's Hospital, Cincinnati OH, 45229-3039, Jeff.Robbins@cchmc.org.

DISCLOSURES

None.

Conclusions: Fibrosis and cardiac dysfunction induced by cardiomyocyte-specific expression of *Mybpc3*^{40kDa} were significantly decreased by *Tgfbr2* ablation in the myofibroblast. Surprisingly, pre-existing fibrosis was partially reversed if the gene was ablated subsequent to fibrotic deposition, suggesting that continued TGFβ signaling through the myofibroblasts was needed to maintain the heart's fibrotic response to a chronic, disease-causing cardiomyocyte-only stimulus.

Keywords

Cardiac myosin binding protein C; transforming growth factor-β; fibrosis; myofibroblast; transgenic model; myocardial fibrosis; TGFβ; Animal Models of Human Disease; Basic Science Research; Cell Signaling/Signal Transduction; Fibrosis

INTRODUCTION

Mutations of cardiac myosin binding protein C (cMyBP-C) account for more than 30% of all identified cardiomyopathy cases.[1–4] About 70% of the identified mutations result in truncated cMyBP-C proteins lacking the C-terminus region.[5] For example, one *Mybpc3* mutation results in a truncated peptide that encodes only the N-terminal 258 amino acids plus 25 additional, new amino acids.[6] Although many of these peptides are unstable and are rapidly turned over,[5] some are relatively long-lived and accumulate in appreciable amounts, functioning as poison peptides.[7] Previously, we found that cardiac stress can trigger cardiac production of a 40kDa cMyBP-C fragment derived from the amino terminus of cMyBP-C (amino acids 1–271) in both human patients and in a mouse surgical model.[8–11] *Mybpc3*^{40kDa} Tg mice expressing the 40kDa fragment specifically in cardiomyocytes developed cardiac hypertrophy, fibrosis and heart failure, mimicking aspects of human disease progression.[11] Subsequent studies identified that the non-canonical TGFβ signaling mitogen activated protein kinase kinase and p38/mitogen activated protein kinase-activated protein kinase 2 pathways were activated in the *Mybpc3*^{40kDa} hearts. Pharmacologically inhibiting either pathway reduced cardiac hypertrophy, alleviated cardiac fibrosis and prolonged survival,[11,12] implicating TGFβ signaling in *Mybpc3*^{40kDa} cardiac disease presentation and progression.

As fibrosis progresses, TGFβ is considered as one of the essential fibrotic signaling ligands that promotes cardiac scar formation.[13] In contrast, bone morphogenetic protein (BMP)7 was identified as an anti-fibrotic counterpart of TGFβ in several organs including the heart.[14–16] Recent studies in the heart suggest that the balance between TGFβ and BMP7 signaling is disrupted in response to disease or after transverse aortic constriction.[16] Activating BMP7 signaling via treatment with recombinant BMP7 or cardiomyocyte-specific knockout of TGFβ receptor II (TβRII) alleviated the cardiac pathology.[15,16]

Cardiac fibrosis can play an important role in cardiac pathogenic processes that occur as a result of acute myocardial infarction or hypertrophic cardiomyopathy. In response to cardiac injury, resident cardiac and smooth muscle α actin (αSMA) fibroblasts are activated and differentiate into myofibroblasts, which are characterized by the expression of cell specific markers such as periostin. Initially, fibrosis is largely an adaptive response, aimed at preserving ventricular wall integrity.[17] With ongoing cardiac dysfunction, fibrosis can continue to progress and transitions into replacement fibrosis, which is associated with

cardiomyocyte loss leading to ventricular dilation and heart failure.[18] Cardiac fibroblast to myofibroblast transition is critical in the activation and progression of cardiac fibrosis in response to pressure overload or genetic hypertrophic cardiomyopathy.[19,20] Additional recent studies suggest that targeting fibroblast or myofibroblast specific fibrotic signaling alleviated cardiac pathology in surgically induced myocardial infarction or pressure-overload mouse models, further indicating a critical role for the fibroblast in cardiac pathological progression.[21–24] However, it is becoming apparent that, rather than being a single process, fibrotic processes and underlying mechanisms are different in response to different cardiac insults. For example, in a previous seminal study, TGFβ neutralized antibody treatment rescued a myosin heavy chain mutation induced hypertrophic cardiomyopathy, but had no effect on TAC surgery induced cardiomyopathy,[15,20] suggesting that the underlying mechanisms may be different. These studies also showed that the cardiomyocyte specific canonical and non-canonical TGFβ signaling behave differently in response to pressure overload versus ischemia reperfusion injury.[15,25] These data are buttressed by more recent studies that suggest fibroblast-specific canonical TGFβ signaling through SMAD3 activation behaves differently in response to TAC and versus ischemia/reperfusion injury.[21,26] because of these potential differences, and in contrast to these prior, acutely induced fibrotic processes, we wished to determine the role TβRII plays in the myofibroblast, but using a genetically-induced, chronic model of cardiomyopathy that undergoes fibrosis over a period of weeks or even months.

TGFis an important cytokine in mediating cardiac fibrosis but may have different roles in the cardiac fibroblast and cardiomyocyte populations and those actions may be cardiac disease-specific and vary over time in the developing disease.[15,20] In the current study, we used a tamoxifen (TAM) inducible myofibroblast-specific Cre recombinase expressing allele[17,21,22] (*Postnmcm*) to create Tg lines in which TβRII could be ablated specifically in the myofibroblast population at early or late times of disease. We crossed these mice into a mouse model that inducibly expressed the pathogenic $Mybpc3^{40kDa}$ allele that generates a unique state of chronic fibrotic disease over time.[11] When the mutant peptide is expressed in cardiomyocytes, cardiac disease accompanied by fibrosis gradually develops.[11] We used these genetic approaches to establish a causal role for excessive myofibroblast activation in this slowly progressive form of genetic cardiomyopathy, a disease that is driven by a cardiomyocyte-intrinsic genetic perturbation and models an important human disease. The importance of myofibroblast TGFβ signaling in mediating a fibrotic response to a sarcomere-based, slowly developing cardiac disease could thus be assessed over time and signaling ablation initiated at different times as well. The data show that continued TGFβ signaling is needed to maintain the degree of fibrosis observed when the ablation was initiated.

METHODS

All supporting data are available within the article.

Animals.—The double transgenic (Dtg) system that allows inducible expression of the 40kDa MyBP-C peptide in cardiomyocytes has been described.[11,27] All crosses were carried out and maintained in the FVB/N background unless otherwise noted.[11] Briefly, the driver

construct (α myosin heavy chain-tetracycline transactivator) was bred with the responder construct that encodes the 40kDa fragment of cMyBP-C. *Mybpc3*^{40kD} expression is induced by withdrawal of doxycycline from the chow. To generate the quadruple compound Tg mice, the *Mybpc3*^{40kDa} Dtg mice were further bred with mice in which a Mer-Cre-Mer cDNA was inserted into the *Postn* (periostin) genetic locus (*Postnmcm)*. Those mice were subsequently bred into *Tgfbr2* floxed (*Tgfbr2*$^{f/f}$ or *r2*$^{f/f}$) mice.[15,17] The *Tgfbr2* floxed and the *Postnmcm* mice were originally made on the C57/B6 background but backcrossed onto the FVB/N background for at least 5 and predominantly 7 generations for the study cohorts. In previous, unpublished studies with the *Mybpc3*^{40kDa} Dtg mice when they were first derived, no gender differences could be detected in terms of pathological remodeling, cardiac function or survival. However, to decrease the total number of mice needed to adequately power the study, only male mice were used except for the final probability of survival curves. To activate *Postnmcm* in myofibroblasts, mice were fed TAM-citrate chow (40 mg/kg body weight, Envigo-TD.130860). For each genotype, each mouse was given a random number, and divided into a control (odd) or TAM (even) group randomly independently of the investigator. Animals were handled in accordance with the principles and procedures of the *Guide for the Care and Use of Laboratory Animals*. All proposed procedures were approved by the Institutional Animal Care and Use Committee at Cincinnati Children's Hospital.

Antibodies and other reagents.—Antibody for (anti-) TGFβ was from Cell signaling (#3711; 1:500 dilution for Western blot). Anti-BMP7 was from Abcam (ab56023; 1:1000 dilution for Western blot). Anti-TGFβRII was from Abcam (ab61213; 1:500 dilution for Western blot). Anti-SMAD3 was from Abcam (ab28379; 1:1000 dilution for Western blot). Anti-phospho-SMAD3 (Ser423/425) was from Cell signaling (#9520; 1:1000 dilution for Western blot). Anti-phospho-SMAD2/3 was from Maine Medical Center Research Institute (D6658; 1:500 dilution for immunofluorescence staining, paraffin section). Anti-SMAD1/5/9 was from Abcam (ab66737; 1:1000 dilution for Western blot). Anti-phospho-SMAD1/5/9 was from Cell Signaling (# 9511; 1:1000 dilution for Western blot). Anti-TAK1 was from Abcam (ab109526; 1:500 dilution for Western blot). Anti-phospho-TAK1 (S412) was from Cell Signaling (#9339; 1:500 dilution for Western blot). Anti-p38 was from Cell Signaling (#9212; 1:1000 dilution for Western blot). Anti-phospho-p38 was from Cell Signaling (#9211; 1:1000 dilution for Western blot). Anti-Myc tag (clone 9E10) was from EMD Millipore (05–419; 1: 1000 dilution for Western blot). Antibody for smooth muscle α actin (-SMA, clone 1A4) was from Sigma-Aldrich (A5228; 1:1000 dilution for Western blot). Anti-troponin I was from EMD Millipore (MAB1691; 1:1000 dilution for immunofluorescence staining, paraffin section). Anti-GAPDH antibody was from EMD Millipore (MAB374, 1:10,000 dilution for Western blot). Wheat germ agglutinin (488) was from ThermoFisher (W11261; 5μg/ml for immunofluorescence staining, paraffin sections).

Histology and immunofluorescent histochemistry.—Hearts were fixed in 10% formalin overnight, and then subjected to a graded series of alcohol dehydrations before being embedded in paraffin blocks for histology. Serial 5-micron sections were collected and subjected to either Masson's trichrome or immunofluorescent staining. For Masson's trichrome staining,5 images per heart were acquired using Olympus BX69 microscope with NIS elements software. The percentage of the blue areas was quantitated as the fibrotic

levels using ImageJ (NIH). For immunofluorescent analyses, antigen retrieval was performed to unmask epitopes. Specifically, deparaffinized sections were boiled in the microwave in 10mM sodium citrate (pH 6.0) buffer for 25 minutes. To validate the specificity of antibodies, a heart section with ischemic/reperfusion was employed as positive control, and a secondary antibody-only section was used as the negative control. Images were acquired using an inverted Nikon A1R confocal microscope equipped with NIS Elements AR 4.13 software. Cardiomyocyte size was determined by wheat germ agglutinin staining. Ten fields per heart were imaged and >1000 cells were quantitated using NIS-Elements software (Nikon). Identities of the paraffin block were blocked to the investigator prior to quantification.

RNA extraction, western blots and hydroxyproline assay.—mRNA was isolated from whole heart or isolated cells using RNAzol-RT reagent (Molecular Research Center) following the manufacturer's protocol. cDNA was generated using iScript cDNA synthesis kit (Bio-Rad) following the manufacturer's protocol. Protein was isolated from whole heart or isolated cells using CellLytic Cell Lysis buffer (Sigma) with protease inhibitor and phosphatase inhibitor cocktail (Roche Diagnostics) following the manufacturer's protocol. Equal amounts of protein were analyzed via SDS gel electrophoresis and Western blots. Hydroxyproline content in left and right ventricular tissue was determined as a measure of fibrosis as described.[28]

Fibroblast isolation.—Adult murine cardiomyocytes and cardiac fibroblasts were isolated as described previously.[17,23] Briefly, beating hearts isolated from anesthetized mice were perfused with modified Tyrode solution supplemented with collagenase II (Worthington). The cardiomyocyte and non-cardiomyocyte fractions were collected after perfusion. To isolate cardiac fibroblasts, endothelial (CD31+) and myeloid (CD45+) cell fractions were sorted from the non-cardiomyocyte fraction using the Magnetic Cell Isolation and Cell Separation kit (Miltenyi Biotec) according to the manufacturer's instructions with antibodies against CD31 (Miltenyi Biotec 130–097-418) and CD45 (Miltenyi Biotec 130–052-301) as described.[17]

Cardiac function.—One percent isoflurane-anesthetized mice were subjected to 2D guided M-mode echocardiography. Left ventricular function was determined using a VisualSonics Vevo 2100 Imaging System with a 40-MHz transducer as described.[12,29] All data were obtained by personnel who were blinded as to genotype and treatment.

Statistical analyses.—Data are expressed as mean±SEM unless otherwise stated. mRNA and protein expression levels were normalized to glyceraldehyde 3-phosphate dehydrogenase (GAPDH). A linear transformation was performed to set the result of control group (usually Ntg without TAM chow) to 1, by dividing each group with the average obtained for their control group. Shapiro-Wilk and Brown-Forsythe tests were performed to examine data normality and variance equality using SigmaPlot V13. The number of mice needed to meet the statistical power (β=0.8) was also calculated using SigmaPlot V13. The following tests were performed using Graphpad (Prism 7). Student's t-test was performed for two group comparisons. A paired t-test was performed to determine the significance of

fractional shortening changes of the same mouse before and after tamoxifen chow treatment. One-way ANOVA with Tukey's post hoc analysis was performed for multiple group comparisons as well as to determine the adjusted *P* value between group comparisons. Kaplan-Meier curves using the Log-rank test were generated to detect changes in survival probabilities. Between group differences were determined using the Holm-Šídák post hoc test. Statistical significance was defined as $*P<0.05$, $**P<0.01$, $***P<0.001$.

RESULTS

TGFβ signaling is activated in the Mybpc3^{40kDa} Tg hearts.

To obtain a profile of fibrotic and TGFβ signaling in the *Mybpc3^{40kDa}* hearts, we analyzed RNA derived from 4-month-old, *Mybpc3^{40kDa}*-expressing hearts using the TGFβ Signaling Targets RT^2 Profiler PCR Array (Qiagen) (Online Supplement, Table I). At this stage, significant cardiac fibrosis is already apparent.[11] We observed that expression of the TGFβ ligands, TGFβ2 and TGFβ3, was significantly induced (Figure 1A). Induction of TGFβ expression was confirmed using Western blots (Online Supplement Figure IA).

Once a TGFβ ligand binds to its heterodimeric receptor complex, TβRI and TβRII, the downstream SMAD-dependent (canonical) and/or SMAD-independent (non-canonical) signaling cascades are activated.[30] While SMAD2 and SMAD3 can sometimes be functionally interchangeable,[31–36] other data suggest that SMAD3 is a more dedicated effector of TGFβ signaling during cardiac fibrosis.[15,21] Hence here we used SMAD3 activation as an indicator of canonical TGFβ signaling. The ratio of the phosphorylated (p) form versus total (t) SMAD3 protein was determined by Western blot (Figure 1B and1C), showing that p-SMAD3 was significantly increased in the *Mybpc3^{40kDa}* hearts compared with controls. p-SMAD3 was dramatically increased in the *Mybpc3^{40kDa}* hearts. Since non-canonical TAK1-p38 signaling can also signal during cardiac fibrosis,[15,22] we determined activated (phosphorylated) (p)-TAK1 levels, which were also significantly upregulated in *Mybpc3^{40kDa}* hearts (Figure 1D and1E). The activation of p38, which is known as a critical TAK1 downstream target in mediating fibrosis[37,38] was also examined. Phosphorylated (p) -p38 was significantly upregulated in *Mybpc3^{40kDa}* hearts compared with controls (Online Supplement Figure IB). The relative increase in p-SMAD2/3 was also detected using immunostaining. Co-immunostaining to detect the affected cell types suggested that the TGFβ signaling was activated in both cardiomyocytes and non-cardiomyocytes (Figure 1F).

BMP7 signaling antagonizes TGFβ signaling through p-SMAD1/5/9.[14,16,39] As fibrosis occurs and progresses, the relative activities of TGFβ and BMP7 signaling can play a significant role in modulating cardiac fibrosis.[15,16] We examined BMP7 mRNA expression in the *Mybpc3^{40kDa}* hearts and found that it was significantly reduced 3 months after *Mybpc3^{40kDa}* expression was initiated (Figure 2A). The reduction of BMP7 was also confirmed via Western blot (Figure 2B). The expression level of another member of the BMP subfamily, BMP4, was also examined but was not changed (Online Supplement Figure II), suggesting that reduced BMP expression was restricted to specific members of the BMP family.

We further analyzed downstream BMP7 signaling through p-SMAD1/5/9. Using phosphorylated (p)-SMAD1/5/9 versus total (t)-SMAD1/5/9 as an indicator, SMAD1/5/9 signaling was also significantly reduced in the Tg mice heart 3 months after *Mybpc3*^{40kDa} expression (Figure 2C).

Fibrotic marker expression is upregulated in the Mybpc3^{40kDa} Tg heart.

We also detected increased RNA expression encoding fibrosis related proteins including connective tissue growth factor, matrix metalloproteinase-14 and tissue inhibitor of metalloproteinase-1 in the Tg hearts 3 months after *Mybpc3*^{40kDa} expression was induced (Figure 3A). We confirmed activation of the transgene using Western blots to detect expression of the c-Myc-tagged Mybpc3^{40kDa} protein (Figure 3B). We also examined the expression of smooth muscle α actin (α-SMA,) a critical myofibroblast marker during the fibroblast to myofibroblast transformation,[40] and noted a two-fold induction of expression as early as 2 months after *Mybpc3*^{40kDa} expression (Figure 3B and 3C).

The extracellular protein periostin is secreted by the activated fibroblasts during fibrosis and is also recognized as an important marker for fibroblast to myofibroblast conversion.[41] The induction of periostin expression could be detected in the Tg hearts as early as one month after *Mybpc3*^{40kDa} expression was initiated (Figure 3D and 3E). By 4 months, periostin could be easily detected both in the perivascular and interstitial space using immunohistochemical staining (Figure 3F).

Myofibroblast specific ablation of Tgfbr2 blocks TGFβ signaling in the activated fibroblasts.

We next examined if we could partially or even completely block fibrosis in the *Mybpc3*^{40kDa} hearts by interfering with TGFβ signaling exclusively within the myofibroblast population. The double-Tg *Mybpc3*^{40kDa} responder mice were crossed to mice containing the TAM-inducible Mer-Cre-Mer cDNA driven off of the myofibroblast-specific Postn (*Postnmcm*) genetic locus as previously described.[17] These triple Tg animals were then bred into *Tgfbr2* floxed animals (*r2*$^{f/f}$)[15] to generate quadruple compound Tg mice (*Mybpc*^{40KDa}*/Postnmcm/r2*$^{f/f}$). To control for even the small chance of a potential impact of mixed strain backgrounds even after >5+ generations of backcrossing into the FVB/N background, the quadruple *Tgfbr2* heterozygous compound Tg mice (*Mybpc*^{40KDa}*/Postnmcm/r2*$^{f/+}$) were included in a control cohort in all subsequent experiments.

To specifically ablate *Tgfbr2* in the myofibroblasts, mice were given TAM-supplemented chow one month after induction of the 40kDa fragment in the cardiomyocytes (Figure 4A). At this stage, the fibrotic response was in its early stages with periostin induction (Figure 3D and 3E). To determine *Tgfbr2* ablation efficiency, cardiac fibroblasts were isolated 4 months after TAM feeding began and expression of the RNA determined. We detected a significant increase of TβRII expression in the fibroblasts isolated from *Mybpc3*^{40kDa} hearts but, in the compound quadruple *Mybpc*^{40KDa}*/Postnmcm/r2*$^{f/f}$ Tg TAM-fed mice, TβRII was significantly reduced (Figure 4B). As it is known that TβRI and TβRII form heterodimers to mediate TGFβ signaling, TβRI expression was also measured. While it was modestly

upregulated in the *Mybpc3*^{40kDa} hearts, no significant differences in TβRI expression were detected between the TAM fed and control groups (Online Supplement Figure IIIA).

We also examined the efficiency of ablation in the isolated cardiac fibroblasts derived from the quadruple *Mybpc*^{40KDa}*/Postnmcm/r2*$^{f/f}$ Tg TAM-fed mice. TβRII protein was reduced approximately 80% in the targeted myofibroblasts (Figure 4C). Along with TβRII depletion, expression of the fibrosis markers, α-SMA and periostin, was also significantly reduced, suggesting that fibrotic signaling was inhibited. Consistent with these data, p-SMAD3 was also decreased (Figure 4D) while p-SMAD1/5/9, was up-regulated (Figure 4E). TAK1 activation was also determined but was not statistically different between the experimental groups (Online Supplement Figure IIIB).

Myofibroblast specific ablation of Tgfbr2 decreases cardiac fibrosis and hypertrophy.

Tgfbr2 myofibroblast ablation had no effect on cardiac levels of Mybpc3^{40KDa} (Online Supplement Figure IVA). We also explored any detrimental effects that tamoxifen feeding might have with respect to sarcomere structure and organization but no obvious changes or pathology using immunohistochemical analyses were detected (Online Supplement Figure IVB), although some hemodynamic effects on the Ntg mice were later noted (Figure 7C).

To rule out any potential confounding data induced by the cell type-specific isolations used in the above experiments, we also determined the effects, if any, of *Tgfbr2* gene dosage on the signaling pathways in the intact heart and quantified p-SMAD3 and p-SMAD1/5/9 levels in 4–5-month-old *Mybpc3*^{40kDa} hearts. p-SMAD3 was significantly induced after 4–5 months, but was inhibited by myoblast-specific *Tgfbr2* ablation, although both alleles needed to be ablated for the levels to approach those observed in the Ntg animals (Figure 5A). p-SMAD1/5/9 anti-fibrotic signaling was significantly up-regulated in the *Tgfbr2* ablated *Mybpc3*^{40kDa} hearts. These data are consistent with a significant decrease of TGF expression and increased BMP7 expression in the myofibroblast-specific *Tgfbr2* ablated *Mybpc3*^{40kDa} hearts (Online Supplement Figure IVC and IVD). We were not able to detect significant activation of the non-canonical signaling pathway as represented by TAK1-p38 signaling (Online Supplement Figure IVE and IVF), suggesting that this pathway may not be active after fibrosis is established in the model. This is consistent with our previous study that non-canonical TGFβ signaling is activated early during fibrosis but is diminished later in the Mybpc3^{40KDa} hearts.[11] Consistent with decreased pro-fibrotic signaling, α-SMA and periostin expression levels were also decreased in the *Tgfbr2* ablated *Mybpc3*^{40kDa} hearts (Figure 5B). Trichrome stained sections derived from the left ventricles (Figure 5C) and the hydroxyproline assay (Online Supplement Figure VA) confirmed that fibrosis was significantly reduced in the *Tgfbr2* ablated *Mybpc3*^{40kDa} hearts relative to the non-ablated, normal chow-fed control mice. Masson's trichrome staining of the right ventricles from *Tgfbr2* ablated *Mybpc3*^{40kDa} hearts also confirmed decreased fibrosis relative to the control group (Online Supplement Figure VC and VD).

Previous data suggest that the fibroblast is essential for cardiac hypertrophy in response to pressure overload.[19] Therefore, we determined whether myofibroblast-specific *Tgfbr*2 ablation impacted on the slowly developing hypertrophic response observed in hearts that expressed Mybpc3^{40kDa} protein over a 3–4 month period. Heart weight to body weight ratios

were measured as an indicator of cardiac hypertrophy (Figure 6A). Compared to the 6-month-old Ntg control group, *Mybpc3^{40kDa}* heart weights were significantly increased, but the rise was reduced in the myofibroblast specific *Tgfbr2* ablated homozygotes compared to *Mybpc3^{40kDa}*-expressing (Dtg) hearts as well as myofibroblast specific *Tgfbr2* ablated heterozygotes (*r2$^{f/+}$*). Cardiomyocyte size was determined directly using wheat germ agglutinin staining in histological sections from the left ventricles (Figure 6B and Online Supplement Figure VB) and right ventricles as well (Online Supplement Figure VE and VF). Myofibroblast *Tgfbr2* ablation resulted in significantly reduced hypertrophy to levels observed in the Ntg hearts. Along with alleviated cardiac hypertrophy, expression of molecular markers of the hypertrophic response, natriuretic peptide A and natriuretic peptide B were determined for the Ntg, Dtg, myofibroblast specific *Tgfbr2* ablated heterozygotes and homozygotes. Only the myofibroblast specific *Tgfbr2* homozygotes showed a significant reduction of natriuretic peptide A and natriuretic peptide B, essentially to normal level (Figure 6C).

Myofibroblast specific ablation of Tgfbr2 preserves cardiac function and prolongs survival.

To determine the impact of myofibroblast specific *Tgfbr2* ablation on cardiac function, transmural echocardiography was performed at both 2 months (Online Supplement Figure VIA, VIB and VIC) and 6 months (Figure 7A, 7B and 7C) of age using echocardiography. As expected, Mybpc3^{40kDa} protein expression over this time span resulted in impaired systolic and diastolic function, the former determined by left ventricular (LV) fractional shortening (FS) and ejection fraction (EF) and the latter by reverse longitudinal strain rate, an index of early diastolic LV filling.[42] Longitudinal fractional shortening (FS) assessment for each mouse in the *Mybpc^{40KDa}/Postnmcm/r2$^{f/f}$* groups demonstrated that myofibroblast-specific *Tgfb2* ablation attenuated the decreased FS that is normally observed in the *Mybpc3^{40kDa}* mice (Online Supplement Figure VID). Plotting FS versus fibrosis percentages identified a moderate negative correlation between the degree of cardiac fibrosis and FS, with the Pearson correlation coefficient = −0.64 and R^2 = 0.73 (Online Supplement Figure VIE). Finally, Kaplan-Meier survival probabilities were determined for all mice in the different experimental cohorts. The data confirmed that ablation of *Tgfbr2* in the myofibroblasts positively impacted on lifespan for more than a year, restoring the probability of survival to essentially those values observed in the Ntg animals (Figure 7D).

Myofibroblast specific ablation of Tgfbr2 reduces pre-existing fibrosis.

Clearly, myofibroblast-specific ablation of TGFβ signaling early in pathogenesis could significantly reduce the fibrotic response and largely prevent cardiac fibrosis from occurring in the face of a chronic, sarcomere-based genetic insult such as *Mybpc3^{40kDa}* cardiomyocyte expression. We wished to determine if a late stage gene ablation of *Tgfbr2* in the myofibroblasts affected fibrosis or cardiac function. After approximately 4 months of *Mybpc3^{40kDa}* cardiomyocyte expression (the mice are 5 months old at this point), there is approximately 20% fibrosis, as determined in our previous study.[12] At this stage, mild systolic dysfunction presents (Figure 8A), while diastolic function is unaffected (Online Supplement Figure VIIA). Ntg and quadruple *Mybpc^{40KDa}/Postnmcm/r2$^{f/f}$* mice were fed with regular or TAM chow beginning 4 months after Mybpc3^{40kDa} expression. After 3 months on TAM chow, TβRII protein was reduced >60% in the isolated fibroblasts and

active p-Smad3 levels were also significantly decreased (Online Supplement Figure VIIB and VIIC, respectively). Although the trend was for TGF to be decreased and anti-fibrotic BMP7 levels increased in the TAM-fed heart lysates relative to hearts derived from the normal chow fed animals, the values did not reach statistical significance (Online Supplement Figure VIID).

Cardiac fibrosis was quantitated in *Mybpc*^{40KDa}*/Postnmcm/r2*$^{f+/+}$ (fed normal chow) and *Mybpc*^{40KDa}*/Postnmcm/r2*$^{f/f}$ (fed TAM chow) groups using both trichrome staining (Figure 8B) and the hydroxyproline assay (Online Supplement Figure VIIIA). Trichrome staining of fibrotic areas was significantly reduced by >50% and hydroxyproline by >75% in the *Tgfbr2* ablated group. To assess the possibility of fibrotic regression, we also compared the TAM chow-fed mice to previously obtained data from the Mybpc^{40kDa} mice, in which fibrosis was quantified after 4 months of Mybpc^{40kDa} expression (5 month-old mice).[12] Compared to these historical controls, trichrome staining of fibrotic areas in the 8-month-old TAM chow-fed mice was reduced by >50%.

Cardiac hypertrophy was examined in the *Mybpc*^{40KDa}*/Postnmcm/r2*$^{f+/+}$ (fed normal chow) and *Mybpc*^{40KDa}*/Postnmcm/r2*$^{f/f}$ (fed TAM chow) groups but there was no significant improvement in the heart weight/body weight ratios (Figure 8C) or decrease in cardiomyocyte size (Online Supplement Figure VIIIB and C). Molecular markers of the hypertrophic response were also examined but we only detected a slight reduction in atrial natriuretic peptide A and no change in atrial natriuretic peptide B (Online Supplement Figure VIIID). The reduction in fibrosis did not rescue the established cardiac hypertrophy but cardiac function was preserved from further decline in the *Tgfbr2* ablated group (Figure 8D and Online Supplement Figure VIIIE). A moderate negative correlation between FS and the degree of fibrosis was apparent (Online Supplement Figure VIIIF). Kaplan-Meier survival curves were also determined for the two experimental groups, as well as for two Ntg group fed, or not fed TAM-supplemented chow and showed that myofibroblast-specific *Tgfbr2* ablation even after cardiac fibrosis was established increased the probability of survival in *Mybpc3*^{40kDa} mice (Figure 8E).

DISCUSSION

A number of structure function studies have centered on mutations in cMyBP-C,[11,43] in which a substantial minority of the mutations causative for human familial hypertrophic cardiomyopathy are found.[44] Those studies led to the finding that an N-terminal fragment of cMyBP-C is found at high levels in human heart failure, is stable, and intercalates into the sarcomere.[8,11] A characteristic of cMyBP-C-based disease is extensive interstitial and perivascular fibrosis and so, we selected this cardiomyocyte-based disease to understand how fibroblast-specific signaling pathways might intersect with and impact upon the chronic fibrotic response induced by cardiomyocyte-specific expression of a pathogenic sarcomere peptide.

Although we have been able to effectively manipulate genetic output in the cardiomyocyte using cell type specific promoters[27,45] we have lacked the molecular and genetic tools to directly manipulate and study the fibroblast's genetic output and contribution to cardiac

disease. With the development of the myofibroblast-specific Postn (*Postnmcm*) genetic locus for driving expression of a tamoxifen inducible Cre allele, it has become possible to directly affect the genetic output of the activated fibroblast both during the induction and early phases of fibrosis.[17,21,22] Thus it is now feasible to explore the consequences of activated fibroblast signaling in the context of the whole heart.

Using these inducible genetic systems, we were able to determine the effects of TGFβ signaling in the myofibroblasts and importantly, at different points in developing cardiac disease. Other than the fibroblasts' role in the elaboration of the extracellular matrix and production of collagen, there is a remarkable lack of data and understanding as to if and how the cells themselves contribute to cardiac disease. Rather, a majority of investigations have been directed at the other cell types in the heart, and particularly, for the familial hypertrophic cardiomyopathies, at the cardiomyocyte, as the bulk of causative mutations lie within the genes that encode the sarcomeric proteins.[46] It should be noted that the inducible system used requires the use of TAM, which can be toxic and, although we noted no overt changes in sarcomere structure (Supplemental Figure IVB), Ntg mice fed a TAM supplemented diet did experience a statistically significant decrease in the reverse peak longitudinal strain rate (Figure 7C). As a TAM supplemented diet was needed for gene ablation, this raises the possibility that the actual degree of functional protection might be greater than the data we were able to obtain show, as some tamoxifen toxicity might have occurred in the treated cohort.

The studies described in this manuscript are directed at understanding and identifying the important signaling pathways within fibroblasts that mediate the development as well the maintenance of longstanding fibrosis in chronic, long term genetically-induced, sarcomere-based cardiac disease. It is important to define the fibrotic consequences of these signaling pathways in the different cardiac cell types as the opposing actions of myofibroblast versus cardiomyocyte SMAD3 signaling have recently been demonstrated in a mouse cardiac infarct model.[21,26] TGFβ signaling is efficiently blunted in the myofibroblasts by the *Tgfbr2*'s ablation and, despite continuous cardiomyocyte-based expression of the primary genetic insult, materially reduced the pathogenic sequelae and significantly increased survival for more than a year. Our study is consistent with recent data showing that fibroblast ablation of the TGFβ receptors alleviated cardiac fibrosis, reduced cardiac hypertrophy, and preserved cardiac function after surgically induced pressure overload.[21] Extending those data, we now show that *Tgfbr2* ablation by itself in the myofibroblast effectively shuts down a pathogenic fibrotic response that normally is triggered during chronic expression of a cardiomyocyte-based pathogenic sarcomeric peptide. We also showed that inducing ablation of TGFβ signaling in the context of established cardiac fibrosis resulted in a significant regression of the fibrotic areas, conserved function and increased survival. These data are consistent with the hypothesis that TGFβ signaling is necessary for the maintenance of fibrosis in the context of this particular disease. These data complement a previous study, which showed that a percentage of cardiac myofibroblasts can convert back to a resident fibroblast program when cardiac stress is removed.[17]

TGFβ signaling has many diverse functions in different cell types and, despite the receptor's ablation at a controlled developmental time in a defined cell type, we cannot rule out off-

target effects that might ultimately affect cardiac function. For example, preliminary surveys indicated the possibility of an altered immune response that might, over a period of time, affect overall cardiovascular health but rigorous exploration of these potential confounding physiological responses will necessarily be the focus of future, more comprehensive studies. Another, potential limitation of this work is that it does not directly measure the number of fibroblasts in the different hearts and so, we are unable to rule out decreased fibroblast expansion over time in the prolonged longitudinal studies. But the functional consequences of *Tgfbr2* are clear in terms of the impact on fibrosis.

We now extend the importance of myofibroblast signaling in the cardiac pathogenic response to a sarcomere-based, chronic genetic stimulus, the presence of the pathogenic MyBP-C 40kDa fragment. Because of TGFβ's involvement in so many fundamental processes, the downstream signal transducers are subject to many potential confounding effects. The need for precise cell type- and temporal control of reductionist gain- and loss-of function studies is underscored by conflicting data on the importance of the different pathways in mediating fibrosis and the cell populations that drive the process. For example, different laboratories have come to different conclusions regarding the necessity or sufficiency of canonical signaling through the SMADs being needed[47] or not for fibrosis.[48] Our data use myofibroblast specific loss of function at different times in order to determine the role of this cell type and the necessity of a pathway in the initiation and maintenance of fibrosis. Studies using timed interventions at precise points in the different cardiac cell types after a signaling pathway's inactivation will be needed in order to more fully understand the complex cell-cell interactions that occur during cardiac fibrosis.

Supplementary Material

Refer to Web version on PubMed Central for supplementary material.

ACKNOWLEDGMENTS

We wish to acknowledge Ms. Victoria Moore (CCHMC) and Ms. Chrissy Schulte (CCHMC) for their expert assistance on analyzing the echocardiographic results.

SOURCES OF FUNDING

This work was supported by National Institutes of Health grants P01HL69779, P01HL059408, R01HL05924, R011062927 and a Trans-Atlantic Network of Excellence grant from Le Fondation Leducq (JR); by American Heart Association Postdoctoral Fellowship grants (QM, BB and IV).

Nonstandard Abbreviations and Acronyms:

BMP	bone morphogenetic protein
cMyBP-C	cardiac myosin binding protein C
Dtg	double transgenic
Mybpc3	cardiac myosin binding protein C gene
GAPDH	glyceraldehyde 3-phosphate dehydrogenase protein

Mybpc3^{40kDa}	40kDa fragment of cMyBP-C
Ntg	Nontransgenic
Postnmcm	periostin allele driving tamoxifen inducible Cre recombinase expression
α-SMA	smooth muscle α actin
p-SMAD	Phosphorylated (activated) SMAD
p-TAK1	Phosphorylated (activated) TGFβ–activated kinase 1
TAM	tamoxifen
Tg	transgenic
TGFβ	transforming growth factor-β
TβRI	TGFβ receptor I protein
TβRII	TGFβ receptor II protein
Tgfbr2	TGFβ receptor II gene
Tgfbr2$^{f/f}$	floxed TGFβ receptor II gene

REFERENCES

1. Erdmann J, Daehmlow S, Wischke S, Senyuva M, Werner U, Raible J, et al. Mutation Spectrum in a Large Cohort of Unrelated Consecutive Patients with Hypertrophic Cardiomyopathy. Clin Genet. 2003;64:339–349. [PubMed: 12974739]
2. Richard P, Charron P, Carrier L, Ledeuil C, Cheav T, Pichereau C, et al. Hypertrophic Cardiomyopathy: Distribution of Disease Genes, Spectrum of Mutations, and Implications for a Molecular Diagnosis Strategy. Circulation. 2003;107:2227–2232. [PubMed: 12707239]
3. Kaski JP, Syrris P, Esteban MT, Jenkins S, Pantazis A, Deanfield JE, et al. Prevalence of Sarcomere Protein Gene Mutations in Preadolescent Children with Hypertrophic Cardiomyopathy. Circ Cardiovasc Genet. 2009;2:436–441. [PubMed: 20031618]
4. Millat G, Bouvagnet P, Chevalier P, Dauphin C, Jouk PS, Da Costa A, et al. Prevalence and Spectrum of Mutations in a Cohort of 192 Unrelated Patients with Hypertrophic Cardiomyopathy. Eur J Med Genet. 2010;53:261–267. [PubMed: 20624503]
5. Barefield D, Sadayappan S. Phosphorylation and Function of Cardiac Myosin Binding Protein-C in Health and Disease. J Mol Cell Cardiol. 2010;48:866–875. [PubMed: 19962384]
6. Carrier L, Bonne G, Bahrend E, Yu B, Richard P, Niel F, et al. Organization and Sequence of Human Cardiac Myosin Binding Protein C Gene (Mybpc3) and Identification of Mutations Predicted to Produce Truncated Proteins in Familial Hypertrophic Cardiomyopathy. Circ Res. 1997;80:427–434. [PubMed: 9048664]
7. Theis JL, Bos JM, Theis JD, Miller DV, Dearani JA, Schaff HV, et al. Expression Patterns of Cardiac Myofilament Proteins: Genomic and Protein Analysis of Surgical Myectomy Tissue from Patients with Obstructive Hypertrophic Cardiomyopathy. Circ Heart Fail. 2009;2:325–333. [PubMed: 19808356]
8. Sadayappan S, Osinska H, Klevitsky R, Lorenz JN, Sargent M, Molkentin JD, et al. Cardiac Myosin Binding Protein C Phosphorylation Is Cardioprotective. Proc Natl Acad Sci U S A. 2006;103:16918–16923. [PubMed: 17075052]

9. Sadayappan S, Gulick J, Klevitsky R, Lorenz JN, Sargent M, Molkentin JD, et al. Cardiac Myosin Binding Protein-C Phosphorylation in a {Beta}-Myosin Heavy Chain Background. Circulation. 2009;119:1253–1262. [PubMed: 19237661]
10. Govindan S, McElligott A, Muthusamy S, Nair N, Barefield D, Martin JL, et al. Cardiac Myosin Binding Protein-C Is a Potential Diagnostic Biomarker for Myocardial Infarction. J Mol Cell Cardiol. 2012;52:154–164. [PubMed: 21971072]
11. Razzaque MA, Gupta M, Osinska H, Gulick J, Blaxall BC, Robbins J. An Endogenously Produced Fragment of Cardiac Myosin-Binding Protein C Is Pathogenic and Can Lead to Heart Failure. Circ Res. 2013;113:553–561. [PubMed: 23852539]
12. Meng Q, Bhandary B, Osinska H, James J, Xu N, Shay-Winkler K, et al. Mmi-0100 Inhibits Cardiac Fibrosis in a Mouse Model Overexpressing Cardiac Myosin Binding Protein C. J Am Heart Assoc. 2017;6.
13. Leask A, Abraham DJ. Tgf-Beta Signaling and the Fibrotic Response. FASEB J. 2004;18:816–827. [PubMed: 15117886]
14. Zeisberg M, Hanai J, Sugimoto H, Mammoto T, Charytan D, Strutz F, et al. Bmp-7 Counteracts Tgf-Beta1-Induced Epithelial-to-Mesenchymal Transition and Reverses Chronic Renal Injury. Nat Med. 2003;9:964–968. [PubMed: 12808448]
15. Koitabashi N, Danner T, Zaiman AL, Pinto YM, Rowell J, Mankowski J, et al. Pivotal Role of Cardiomyocyte Tgf-Beta Signaling in the Murine Pathological Response to Sustained Pressure Overload. J Clin Invest. 2011;121:2301–2312. [PubMed: 21537080]
16. Merino D, Villar AV, Garcia R, Tramullas M, Ruiz L, Ribas C, et al. Bmp-7 Attenuates Left Ventricular Remodelling under Pressure Overload and Facilitates Reverse Remodelling and Functional Recovery. Cardiovasc Res. 2016;110:331–345. [PubMed: 27068510]
17. Kanisicak O, Khalil H, Ivey MJ, Karch J, Maliken BD, Correll RN, et al. Genetic Lineage Tracing Defines Myofibroblast Origin and Function in the Injured Heart. Nat Commun. 2016;7:12260. [PubMed: 27447449]
18. Stempien-Otero A, Kim DH, Davis J. Molecular Networks Underlying Myofibroblast Fate and Fibrosis. J Mol Cell Cardiol. 2016;97:153–161. [PubMed: 27167848]
19. Takeda N, Manabe I, Uchino Y, Eguchi K, Matsumoto S, Nishimura S, et al. Cardiac Fibroblasts Are Essential for the Adaptive Response of the Murine Heart to Pressure Overload. J Clin Invest. 2010;120:254–265. [PubMed: 20038803]
20. Teekakirikul P, Eminaga S, Toka O, Alcalai R, Wang L, Wakimoto H, et al. Cardiac Fibrosis in Mice with Hypertrophic Cardiomyopathy Is Mediated by Non-Myocyte Proliferation and Requires Tgf-Beta. J Clin Invest. 2010;120:3520–3529. [PubMed: 20811150]
21. Khalil H, Kanisicak O, Prasad V, Correll RN, Fu X, Schips T, et al. Fibroblast-Specific Tgf-Beta-Smad2/3 Signaling Underlies Cardiac Fibrosis. J Clin Invest. 2017;127:3770–3783. [PubMed: 28891814]
22. Molkentin JD, Bugg D, Ghearing N, Dorn LE, Kim P, Sargent MA, et al. Fibroblast-Specific Genetic Manipulation of P38 Mitogen-Activated Protein Kinase in Vivo Reveals Its Central Regulatory Role in Fibrosis. Circulation. 2017;136:549–561. [PubMed: 28356446]
23. Travers JG, Kamal FA, Valiente-Alandi I, Nieman ML, Sargent MA, Lorenz JN, et al. Pharmacological and Activated Fibroblast Targeting of Gbetagamma-Grk2 after Myocardial Ischemia Attenuates Heart Failure Progression. J Am Coll Cardiol. 2017;70:958–971. [PubMed: 28818206]
24. Xiang FL, Fang M, Yutzey KE. Loss of Beta-Catenin in Resident Cardiac Fibroblasts Attenuates Fibrosis Induced by Pressure Overload in Mice. Nat Commun. 2017;8:712. [PubMed: 28959037]
25. Rainer PP, Hao S, Vanhoutte D, Lee DI, Koitabashi N, Molkentin JD, et al. Cardiomyocyte-Specific Transforming Growth Factor Beta Suppression Blocks Neutrophil Infiltration, Augments Multiple Cytoprotective Cascades, and Reduces Early Mortality after Myocardial Infarction. Circ Res. 2014;114:1246–1257. [PubMed: 24573206]
26. Kong P, Shinde AV, Su Y, Russo I, Chen B, Saxena A, et al. Opposing Actions of Fibroblast and Cardiomyocyte Smad3 Signaling in the Infarcted Myocardium. Circulation. 2017;137:707–724. [PubMed: 29229611]

27. Sanbe A, Gulick J, Hanks MC, Liang Q, Osinska H, Robbins J. Reengineering Inducible Cardiac-Specific Transgenesis with an Attenuated Myosin Heavy Chain Promoter. Circ Res. 2003;92:609–616. [PubMed: 12623879]
28. Accornero F, van Berlo JH, Correll RN, Elrod JW, Sargent MA, York A, et al. Genetic Analysis of Connective Tissue Growth Factor as an Effector of Transforming Growth Factor Beta Signaling and Cardiac Remodeling. Mol Cell Biol. 2015;35:2154–2164. [PubMed: 25870108]
29. Bhuiyan MS, McLendon P, James J, Osinska H, Gulick J, Bhandary B, et al. In Vivo Definition of Cardiac Myosin-Binding Protein C's Critical Interactions with Myosin. Pflugers Arch. 2016;468:1685–1695. [PubMed: 27568194]
30. Massague J Tgfbeta Signalling in Context. Nat Rev Mol Cell Biol. 2012;13:616–630. [PubMed: 22992590]
31. Souchelnytskyi S, Tamaki K, Engstrom U, Wernstedt C, ten Dijke P, Heldin CH. Phosphorylation of Ser465 and Ser467 in the C Terminus of Smad2 Mediates Interaction with Smad4 and Is Required for Transforming Growth Factor-Beta Signaling. J Biol Chem. 1997;272:28107–28115. [PubMed: 9346966]
32. Massague J, Seoane J, Wotton D. Smad Transcription Factors. Genes Dev. 2005;19:2783–2810. [PubMed: 16322555]
33. Schmierer B, Hill CS. Kinetic Analysis of Smad Nucleocytoplasmic Shuttling Reveals a Mechanism for Transforming Growth Factor Beta-Dependent Nuclear Accumulation of Smads. Mol Cell Biol. 2005;25:9845–9858. [PubMed: 16260601]
34. Liu Y, Festing M, Thompson JC, Hester M, Rankin S, El-Hodiri HM, et al. Smad2 and Smad3 Coordinately Regulate Craniofacial and Endodermal Development. Dev Biol. 2004;270:411–426. [PubMed: 15183723]
35. Shen X, Hu PP, Liberati NT, Datto MB, Frederick JP, Wang XF. Tgf-Beta-Induced Phosphorylation of Smad3 Regulates Its Interaction with Coactivator P300/Creb-Binding Protein. Mol Biol Cell. 1998;9:3309–3319. [PubMed: 9843571]
36. Dunn NR, Koonce CH, Anderson DC, Islam A, Bikoff EK, Robertson EJ. Mice Exclusively Expressing the Short Isoform of Smad2 Develop Normally and Are Viable and Fertile. Genes Dev. 2005;19:152–163. [PubMed: 15630024]
37. Bujak M, Frangogiannis NG. The Role of Tgf-Beta Signaling in Myocardial Infarction and Cardiac Remodeling. Cardiovasc Res. 2007;74:184–195. [PubMed: 17109837]
38. Wang L, Ma R, Flavell RA, Choi ME. Requirement of Mitogen-Activated Protein Kinase Kinase 3 (Mkk3) for Activation of P38alpha and P38delta Mapk Isoforms by Tgf-Beta 1 in Murine Mesangial Cells. J Biol Chem. 2002;277:47257–47262. [PubMed: 12374793]
39. Weiskirchen R, Meurer SK. Bmp-7 Counteracting Tgf-Beta1 Activities in Organ Fibrosis. Front Biosci (Landmark Ed). 2013;18:1407–1434. [PubMed: 23747893]
40. Hinz B, Gabbiani G. Mechanisms of Force Generation and Transmission by Myofibroblasts. Curr Opin Biotechnol. 2003;14:538–546. [PubMed: 14580586]
41. Tallquist MD, Molkentin JD. Redefining the Identity of Cardiac Fibroblasts. Nat Rev Cardiol. 2017;14:484–491. [PubMed: 28436487]
42. Schnelle M, Catibog N, Zhang M, Nabeebaccus AA, Anderson G, Richards DA, et al. Echocardiographic Evaluation of Diastolic Function in Mouse Models of Heart Disease. J Mol Cell Cardiol. 2018;114:20–28. [PubMed: 29055654]
43. Sadayappan S, Gulick J, Osinska H, Martin LA, Hahn HS, Dorn GW, 2nd, et al. Cardiac Myosin-Binding Protein-C Phosphorylation and Cardiac Function. Circ Res. 2005;97:1156–1163. [PubMed: 16224063]
44. Carrier L, Mearini G, Stathopoulou K, Cuello F. Cardiac Myosin-Binding Protein C (Mybpc3) in Cardiac Pathophysiology. Gene. 2015;573:188–197. [PubMed: 26358504]
45. Gulick J, Hewett TE, Klevitsky R, Buck SH, Moss RL, Robbins J. Transgenic Remodeling of the Regulatory Myosin Light Chains in the Mammalian Heart. Circ Res. 1997;80:655–664. [PubMed: 9130446]
46. Marian AJ, Braunwald E. Hypertrophic Cardiomyopathy: Genetics, Pathogenesis, Clinical Manifestations, Diagnosis, and Therapy. Circ Res. 2017;121:749–770. [PubMed: 28912181]

47. Oka T, Xu J, Kaiser RA, Melendez J, Hambleton M, Sargent MA, et al. Genetic Manipulation of Periostin Expression Reveals a Role in Cardiac Hypertrophy and Ventricular Remodeling. Circ Res. 2007;101:313–321. [PubMed: 17569887]

48. Niculescu-Duvaz I, Phanish MK, Colville-Nash P, Dockrell ME. The Tgfbeta1-Induced Fibronectin in Human Renal Proximal Tubular Epithelial Cells Is P38 Map Kinase Dependent and Smad Independent. Nephron Exp Nephrol. 2007;105:e108–116. [PubMed: 17347580]

NOVELTY AND SIGNIFICANCE

What Is Known?

- During the development of cardiac disease, fibrosis can contribute to the developing pathology and activation of cardiac Transforming Growth Factor beta (TGFβ) plays an important role in these processes.
- Targeting fibroblast or myofibroblast specific TGFβ signaling reduces cardiac pathogenic fibrosis in surgically induced myocardial infarction or pressure-overload rodent models

What New Information Does This Article Contribute?

- Using a chronic, genetically induced model of cardiac disease and fibrosis induced by cardiomyocyte-specific expression of a cardiac myosin binding protein C fragment, we ablated TGFβ signaling only in the myofibroblasts and showed that TGFβ signaling in that cell type is necessary for fibrosis to occur.
- By inducing and then later ablating myofibroblast-based, TGFβ signaling after fibrosis was established, we demonstrated that TGFβ signaling is required for myofibroblast and fibrotic maintenance, as fibrosis could be partially reversed if TGFβ signaling was stopped after extensive fibrosis had occurred.

Cardiac myosin binding protein C (cMyBP-C) mutations are responsible for approximately 30% of genetically identified cardiomyopathies in human patients. As many of the mutations result in truncated protein, the pathology is often ascribed to haploinsufficiency but in some circumstances, the protein fragment is stable and can act as a poison peptide. Previously, we identified a cMyBP-C 40KDa protein fragment derived from the n amino-terminus. The fragment was present in human heart failure and, when expressed specifically in cardiomyocytes in the mouse heart, caused cardiac disease, fibrosis and eventual heart failure. Using cardiomyocyte-specific, inducible transgenesis, expression of the mutant peptide could be induced or inactivated by pharmacological means and we used this system to explore the cell-specific necessity of TGFβ signaling in cardiac fibrosis, by breeding these mice to mice in which we could inducibly ablate a protein critical for TGFβ activation, TGFβ receptor II specifically in activated myofibroblasts. This genetic approach allowed us to explore the consequences of specifically ablating TGFβ signaling in the myofibroblast during fibrosis to understand the pathway's role in fibrotic processes initiated by changes in the cardiomyocyte. We discovered that, in a chronic genetic model of cardiomyocyte-based disease, myofibroblast-restricted signaling is essential for both the initiation and maintenance of pathogenic fibrosis.

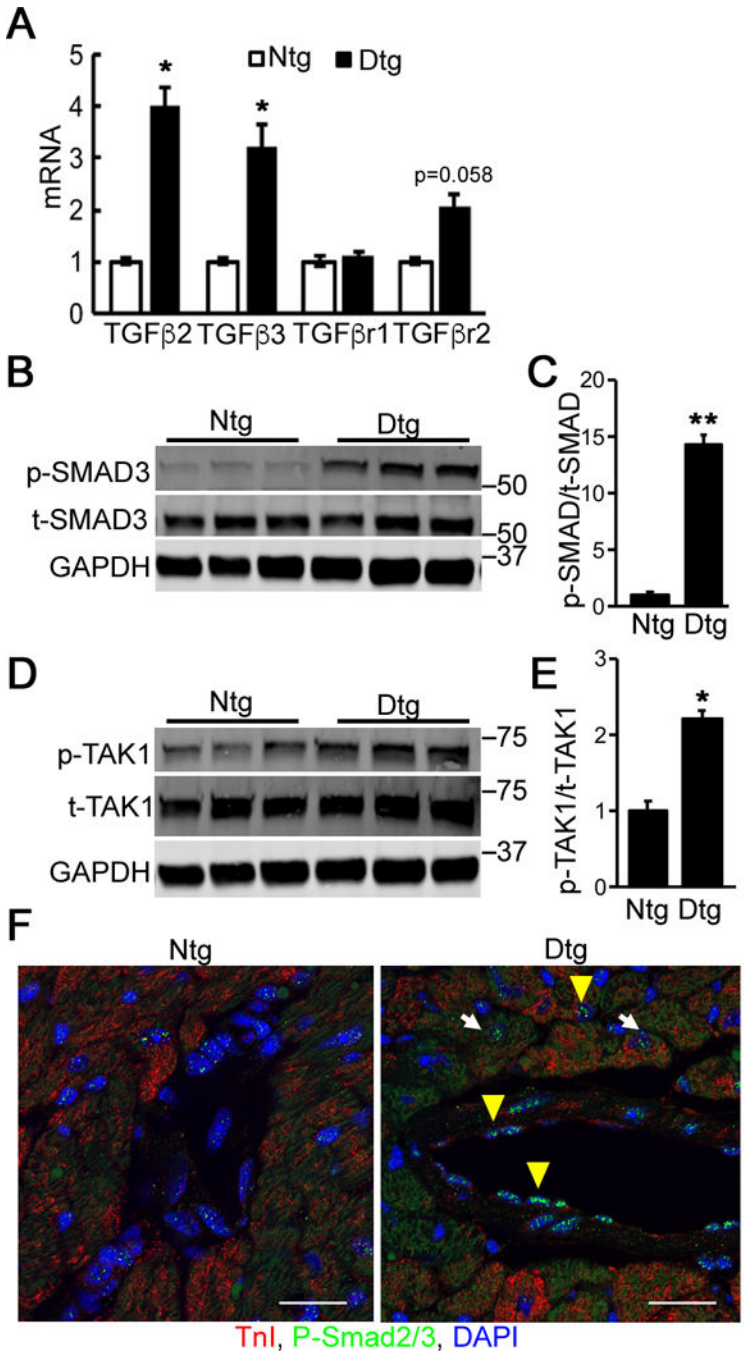

Figure 1. TGFβ signaling is activated in *Mybpc3*^{40kDa} hearts.

A, RNA levels were determined via quantitative RT-PCR for TGFβ ligands and receptors in nontransgenic (Ntg)- and *Mybpc3*^{40kDa}-expressing (Dtg) heart lysates. TGFβ receptor I and II (TβRI and TβRII, respectively), n=3. **B,** Activation of SMAD3 signaling was detected using Western blot analyses of total cardiac protein. **C,** The ratio of phosphorylated (p)-SMAD3 to total (t)-SMAD3 was determined from the Western blot, n=4. **D,** TAK1 levels were determined using Western blot analyses of total cardiac protein. **E,** The ratio of phosphorylated (p)-TAK1 to total (t)-TAK1 was determined from the Western blot, n=6. **F,**

Immunostaining for p-SMAD2/3 (green) in Ntg and Dtg heart sections derived from the left ventricles. DAPI (blue) was used to detect nuclei and troponin I (red) identified cardiomyocytes. White arrow: p-SMAD2/3 positive cardiomyocyte; yellow arrowhead: p-SMAD3 positive non-cardiomyocyte. Scale bar: 25 μm. Data normalization and between group differences analysis were performed as described in **Methods**. *$P<0.05$, **$P<0.01$. All samples were derived from 4-month-old mice (3 months after withdrawal of doxycycline to activate Mybpc3^{40kDa} protein expression).

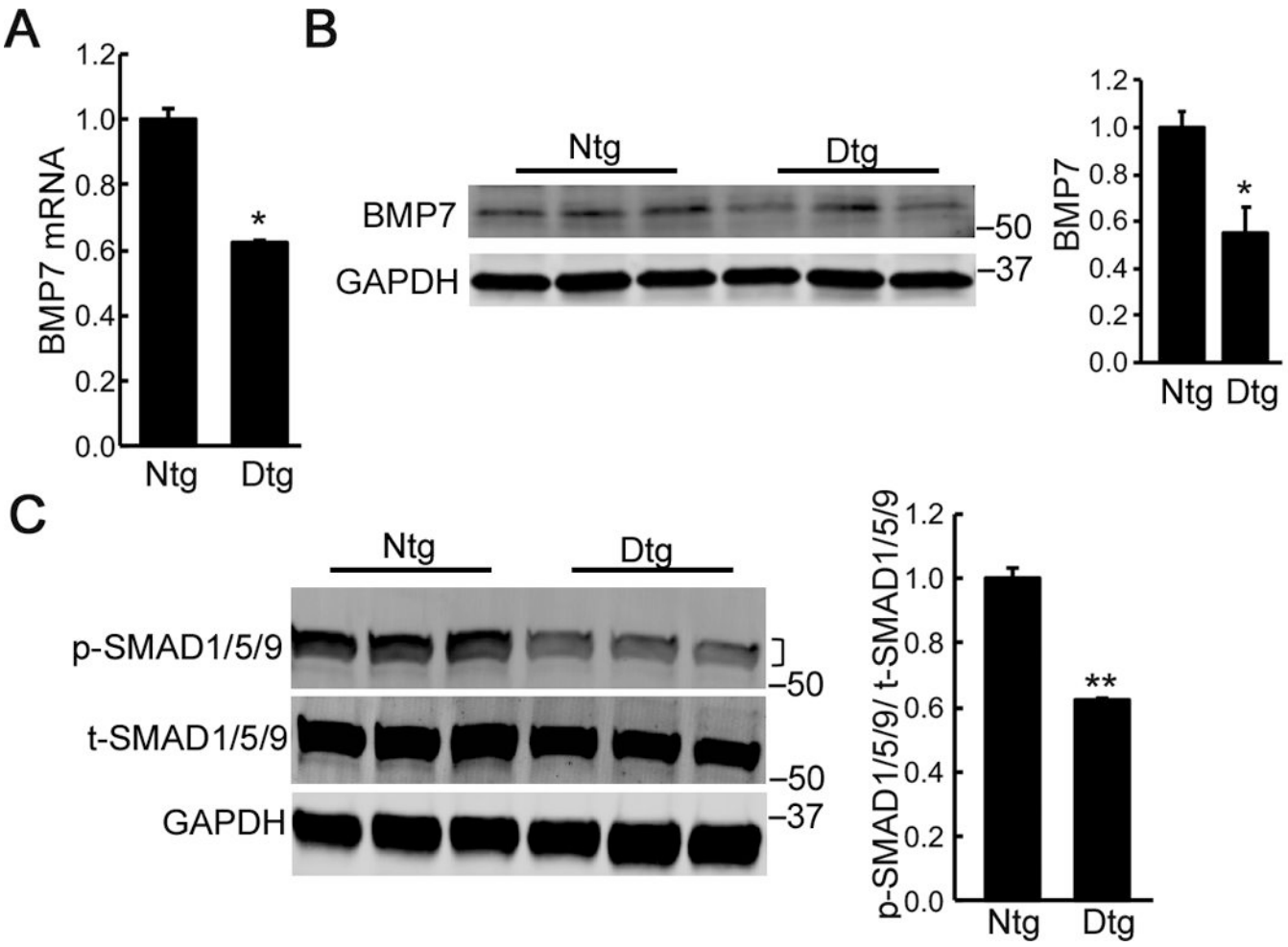

Figure 2. BMP7 signaling is inhibited in *Mybpc3*^{40kDa} hearts. Samples were derived from 4-month-old nontransgenic (Ntg)- and *Mybpc3*^{40kDa}-expressing (Dtg) hearts treated as described in Figure 1.

A, Reduced expression of BMP7 was detected in Dtg hearts using quantitative RT-PCR and **B,** Western blot after Mybpc3^{40kDa} protein expression for 3 months. **C,** Decreased SMAD1/5/9 signaling was detected using Western blot analyses of total cardiac protein. The ratio of phosphorylated (p)-SMAD1/5/9 to total (t)-SMAD1/5/9 was determined from the Western blot. A bracket, where present, indicates the area used for quantitation. Data normalization and between group differences analysis were performed as described in **Methods**. n=4, *P<0.05, **P<0.01.

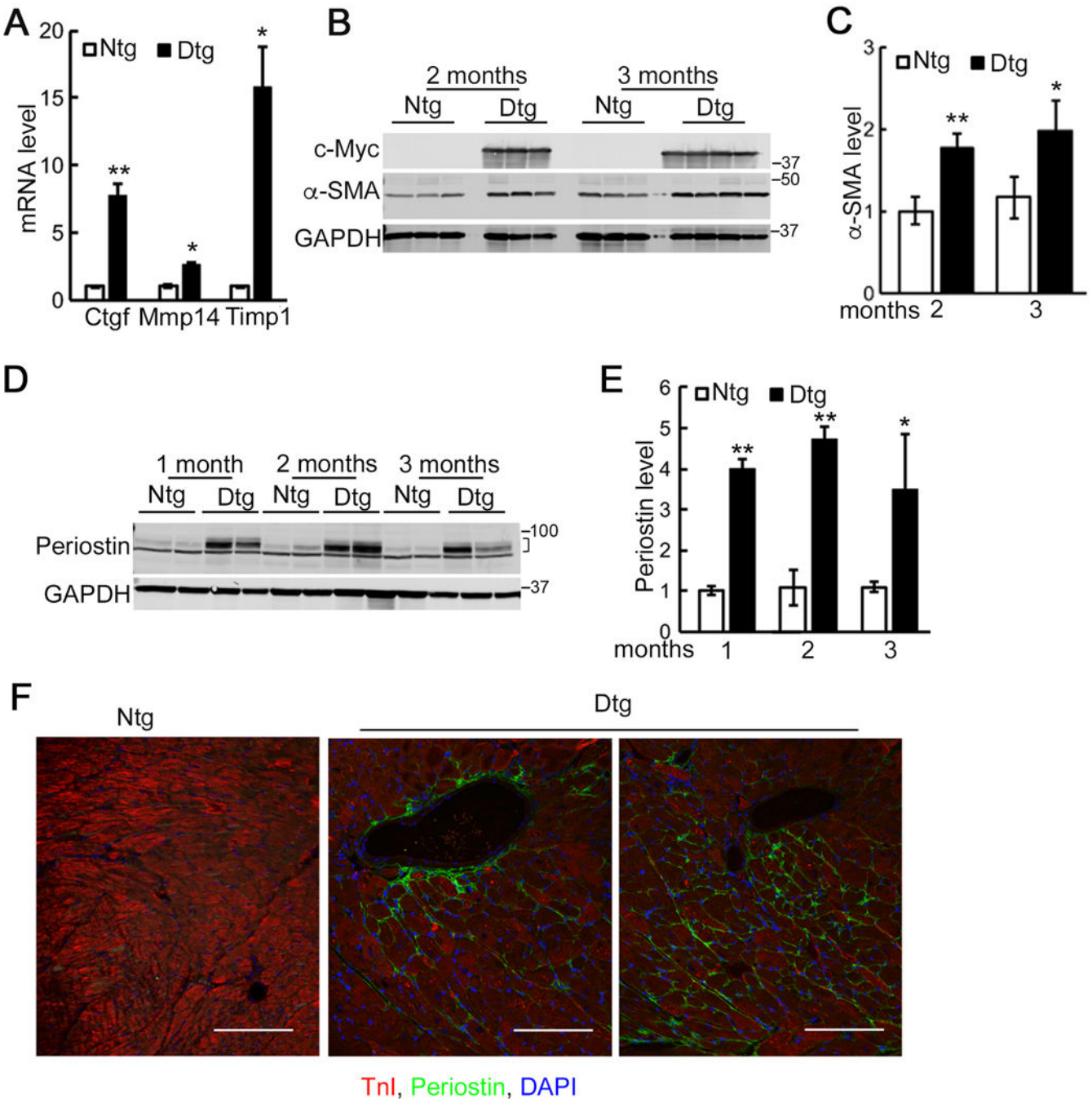

Figure 3. Expression of fibrotic markers in *Mybpc3*^{40kDa}-expressing (Dtg) hearts.

A, Quantitative RT-PCR analysis of selected fibrotic markers in control (Ntg) and Dtg heart lysates after 3 months of Mybpc3^{40kDa} protein expression, which was induced at 1 month by withdrawal of doxycycline from the chow, n=3. Connective tissue growth factor, matrix metalloproteinase-14 and tissue inhibitor of metalloproteinase-1 (Ctgf, Mmp14 and Timp1, respectively). **B,** Western blot analysis confirmed expression of the c-Myc-tagged *Mybpc3*^{40kDa} protein. Increased expression of smooth muscle α actin (α-SMA) was also detected in Western blot analyses of total cardiac protein. **C,** Quantitation of α-SMA from

the Western blot. Data are expressed as mean ± SD, n=4. **D,** Increased expression of periostin was detected using Western blot analyses of total cardiac protein. **E,** Quantitation of the Western blot. Data are expressed as mean ± SD, n=4. A bracket, where present, indicates the area used for quantitation. **F,** Periostin (green) in Ntg and Dtg hearts at 4 months of age. Blue, DAPI (nucleic acid); red, troponin I (cardiomyocytes). Scale bar: 100 μm. Data normalization and between group differences analysis were performed as described in **Methods**. *P<0.05, **P<0.01.

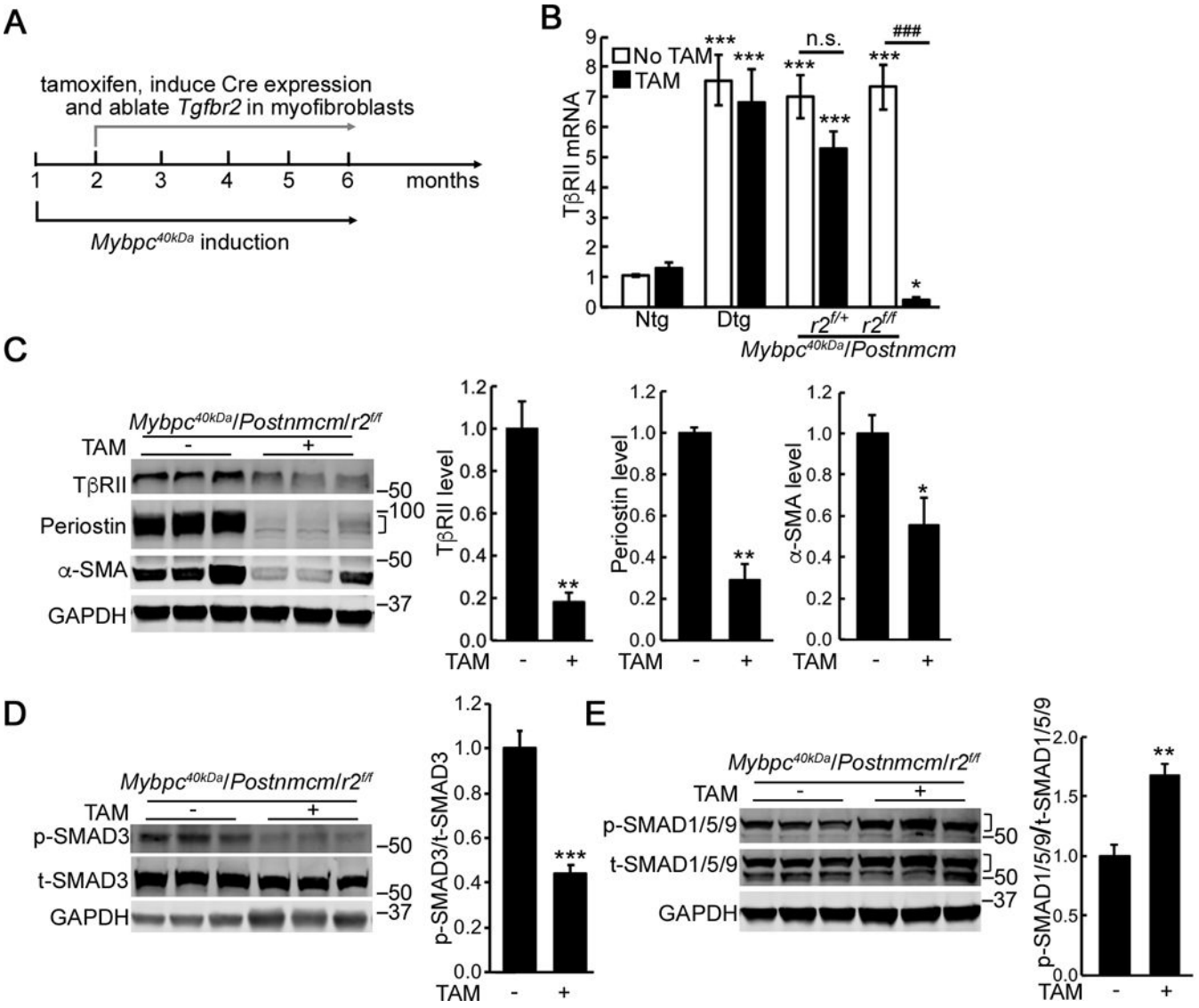

Figure 4. Myofibroblast specific ablation of *Tgfbr2* (*r2*).

A, Schematic diagram of the experimental design. To ablate *Tgfbr2* in the quadruple Tg mice, experimental groups were given tamoxifen (TAM) chow for 1 month after transgene induction at 2 months of age. **B,** Reduced *r2* expression was detected in cardiac fibroblasts isolated from the *Mybpc^{40kDa}/Postnmcm/r2$^{f/f}$* mice on TAM chow. One-way ANOVA analysis with Tukey's post hoc test, **P*<0.05, ****P*<0.001, compared to the Ntg, no TAM group; $^{###}$*P*<0.001, between group comparison, n=4. **C**, Reduced expression of TβRII, α-SMA and periostin occurred in cardiac fibroblasts isolated from the *Mybpc^{40kDa}/Postnmcm/r2$^{f/f}$* mice fed with TAM chow. Between group comparisons, n=4, **P*<0.05, ***P*<0.01. **D,** Reduced p-SMAD3 signaling (n=7) and **E,** increased p-SMAD1/5/9 signaling (n=4) were detected in cardiac fibroblasts isolated from the *Mybpc^{40kDa}/Postnmcm/r2$^{f/f}$* mice fed with TAM chow. Between group comparison, **P*<0.05, ***P*<0.01. Mybpc3^{40kDa} expression was induced at 1 month, Postnmcm was activated at 2 months by feeding TAM chow, and mice harvested at 6 months of age. Data normalization was performed as

described in **Methods**. Groups were: Ntg; nontransgenic, Dtg; *Mybpc3*^{40kDa}-expressing hearts, *Mybpc*^{40kDa}*/Postnmcm/r2*$^{f/+}$; *Mybpc3*^{40kDa}*/Postnmcm/Tgfbr2*$^{f/+}$, *Mybpc*^{40kDa}*/Postnmcm/r2*$^{f/f}$; *Mybpc3*^{40kDa}*/Postnmcm/Tgfbr2*$^{f/f}$. A bracket, where present, indicates the area used for quantitation.

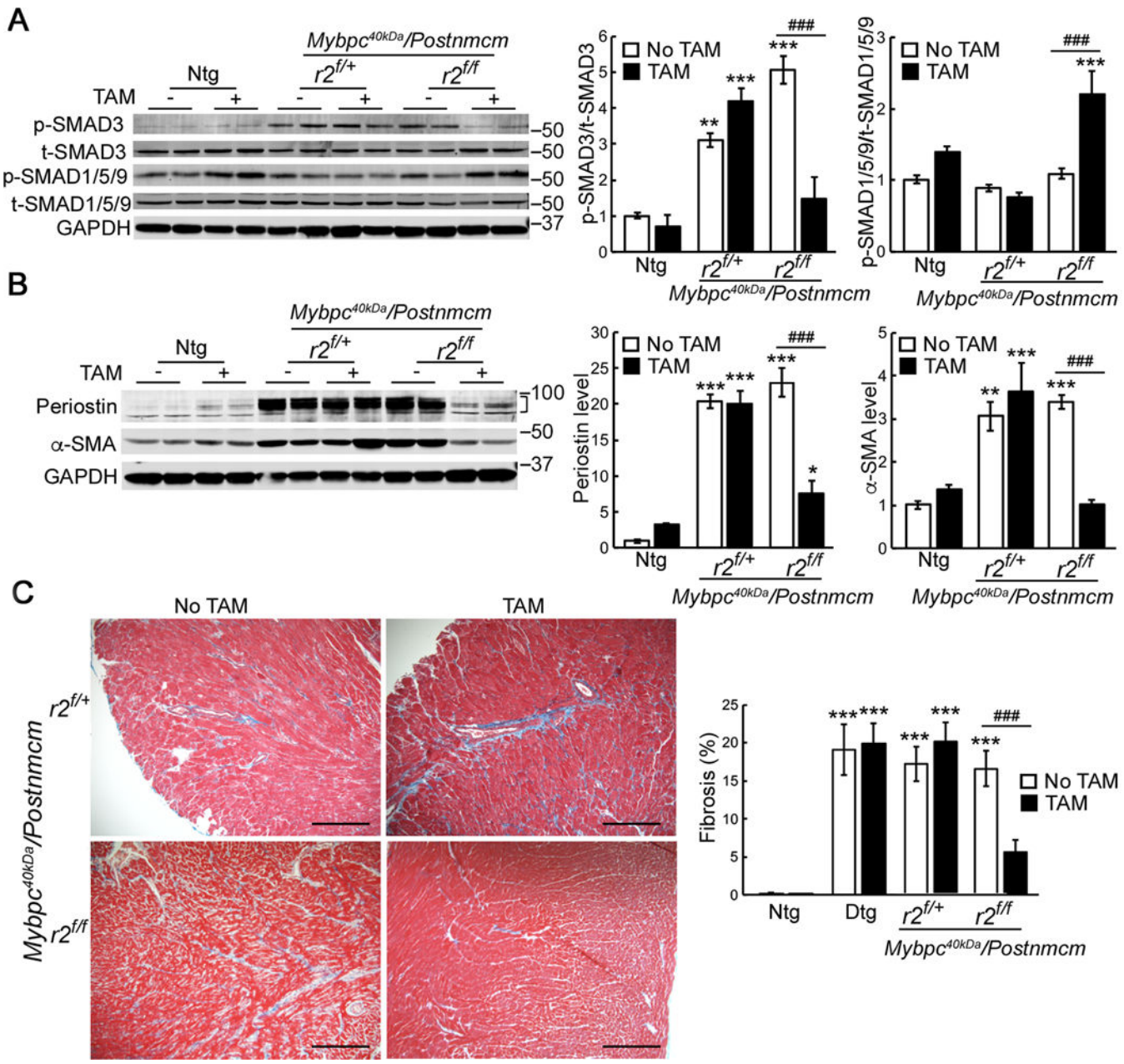

Figure 5. Myofibroblast specific ablation of *Tgfbr2* (*r2*) reduces cardiac fibrosis in *Mybpc3*^{40kDa} hearts.

A, Reduced p-SMAD3 signaling and increased p-SMAD1/5/9 signaling **B,** Reduced expression of smooth muscle α actin (α-SMA) and periostin were detected in heart lysates isolated from *Mybpc*^{40kDa}*/Postnmcm/r2*$^{f/f}$ mice fed with tamoxifen (TAM) chow compared to normal chow. n=3 for Ntg groups, n=4 for other groups. A bracket, where present, indicates the area used for quantitation. **C,** Representative left ventricle sections subjected to Masson's trichrome staining. The *Mybpc*^{40kDa}*/Postnmcm/r2*$^{f/+}$ *and Mybpc*^{40kDa}*/Postnmcm/r2*$^{f/f}$ hearts are shown. Scale bar: 10X, 500 μm. The degree of fibrosis was quantitated, n=6 for Ntg groups, n=3 for Dtg groups, n=4 for other groups. One-way ANOVA analysis with Tukey's post hoc test, **P*<0.05, ***P*<0.01, ****P*<0.001, comparing to

nontransgenic (Ntg), normal chow group; $^{###}P<0.001$, between group comparison. Data normalization was performed as described in **Methods**. Mybpc3^{40kDa} expression was induced at 1 month, Postnmcm was activated at 2 months by feeding TAM chow, and mice harvested at 6–7 months of age.

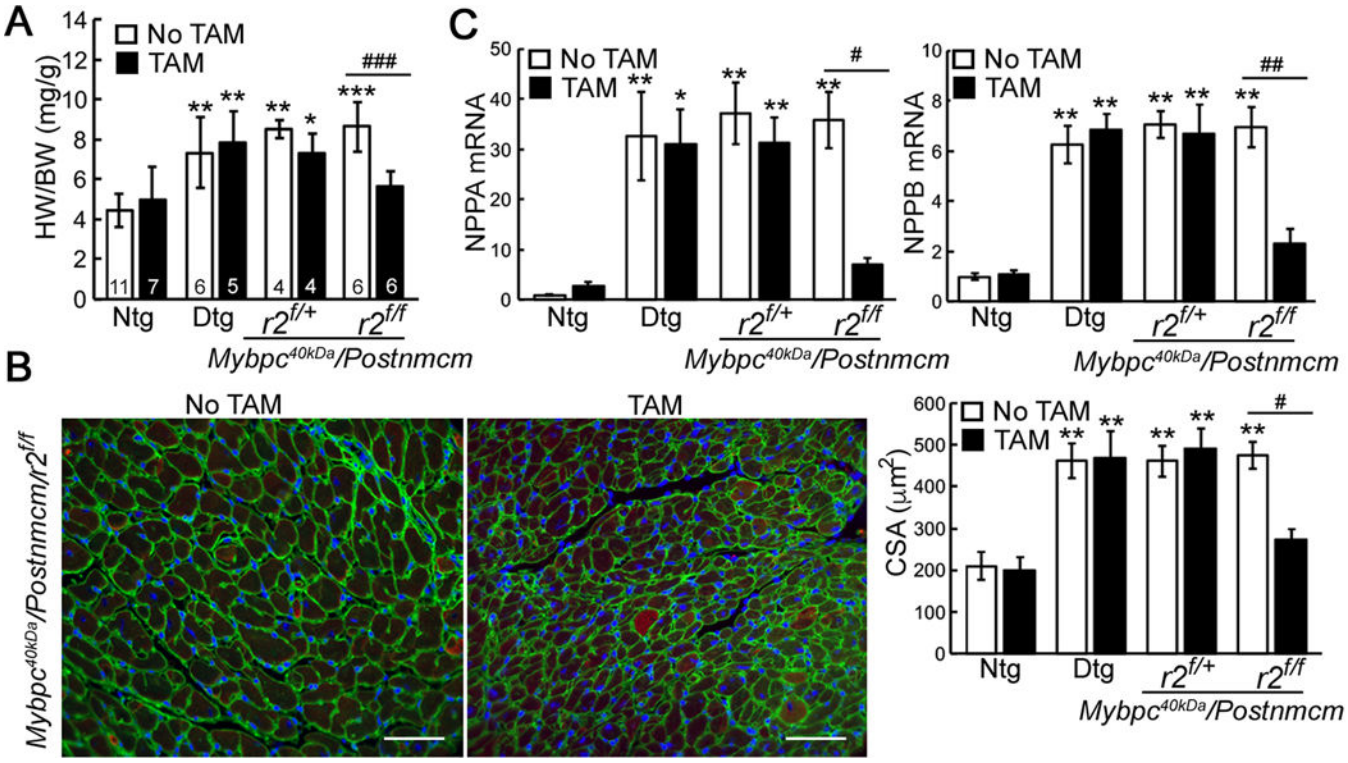

Figure 6. Myofibroblast ablation of *Tgfbr2* (*r2*) decreases *Mybpc3*^{40kDa}-induced cardiac hypertrophy.

A, Heart weight (HW) to body weight (BW) ratios in the control and experimental cohorts. Six-month-old nontransgenic (Ntg)- and *Mybpc3*^{40kDa}-expressing (Dtg) hearts were analyzed as well as heterozygote (*r2*$^{f/+}$) and homozygote (*r2*$^{f/f}$) nulls of *Tgfbr2* crossed into the Dtg background. Data are expressed as mean ± SD, n=4–11. **B,** Wheat germ agglutinin (green) staining on samples derived from the left ventricles was used to determine the cross-sectional area (CSA) of the cardiomyocytes, n=4. Scale bar=50 μm. No significant changes were detected between the TAM-fed Ntg and *Mybpc*^{40kDa}/*Postnmcm*/*r2*$^{f/f}$ groups, adjusted *P*=0.9008. **C,** Natriuretic peptide A and B (Nppa and Nppb, respectively) mRNA expression, n=4. One-way ANOVA analysis with Tukey's post hoc test, **P*<0.05, ***P*<0.01, ****P*<0.001comparing the indicated genotypes to the Ntg, no TAM group. $^{\#}$*P*<0.05, $^{\#\#}$*P*<0.01, $^{\#\#\#}$*P*<0.001 between group comparison. Whole ventricle lysates were used for these experiments. Data normalization was performed as described in **Methods**.

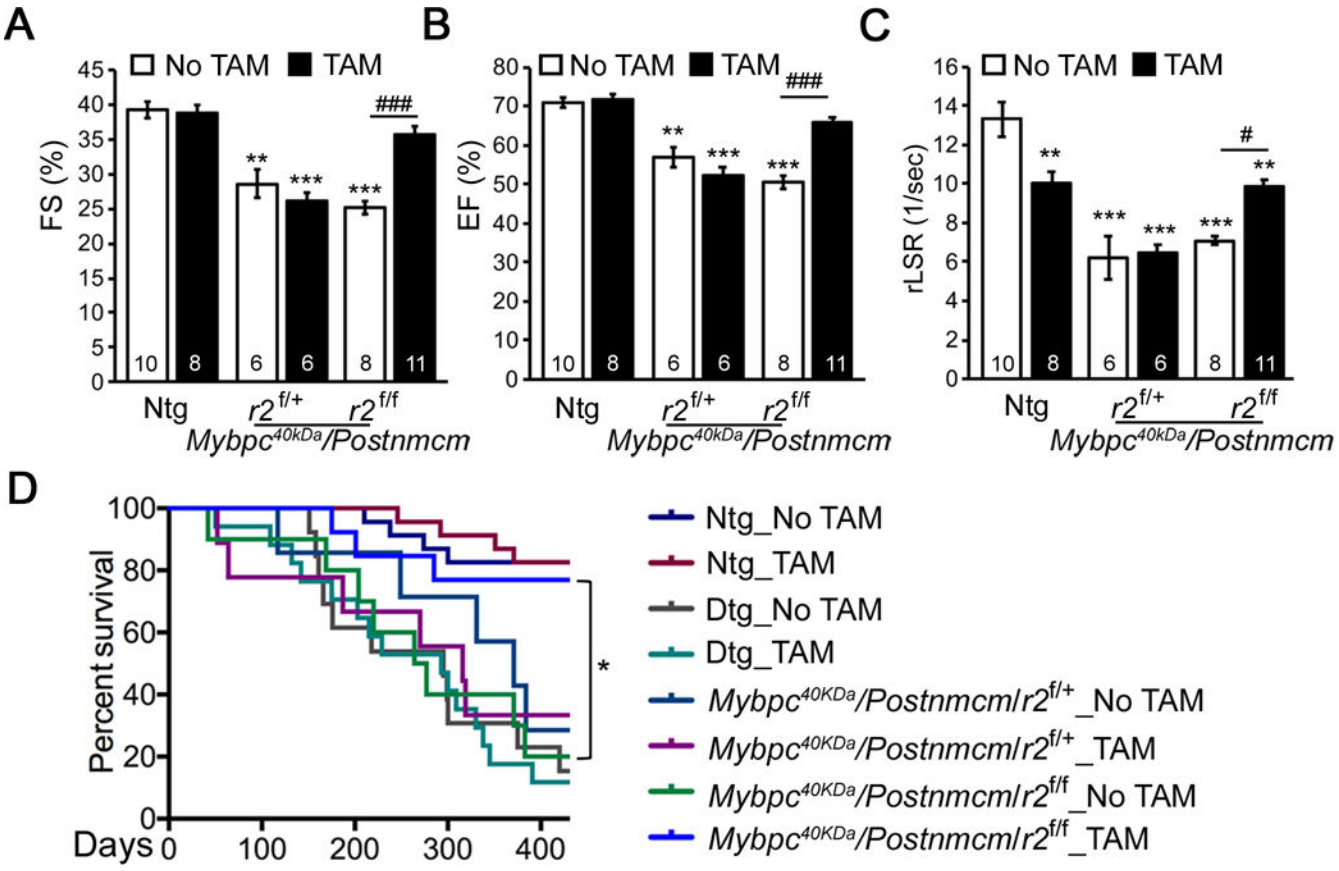

Figure 7. Myofibroblast specific ablation of *Tgfbr2* (*r2*) preserves cardiac function and prolongs *Mybpc3*^{40kDa} mouse survival.

A-C, Echocardiographic analyses of 6-month-old nontransgenic (Ntg)- and *Mybpc3*^{40kDa}-expressing (Dtg) hearts as well as heterozygote (*r2*$^{f/+}$) and homozygote (*r2*$^{f/f}$) nulls of *Tgfbr2* crossed into the Dtg background. One-way ANOVA analysis with Tukey's post hoc test, ** P<0.01, *** P<0.001, comparing to Ntg, no tamoxifen (TAM) group; ### P<0.001, between group comparison, n=6–11. **D**, Kaplan-Meier survival curve. P<0.0001 using the Log-rank test, n=7–23; all between group comparisons were performed using the Holm-Šídák post hoc test, * P<0.05. FS; fractional shortening, EF; ejection fraction, rLSR; reverse peak longitudinal strain rate.

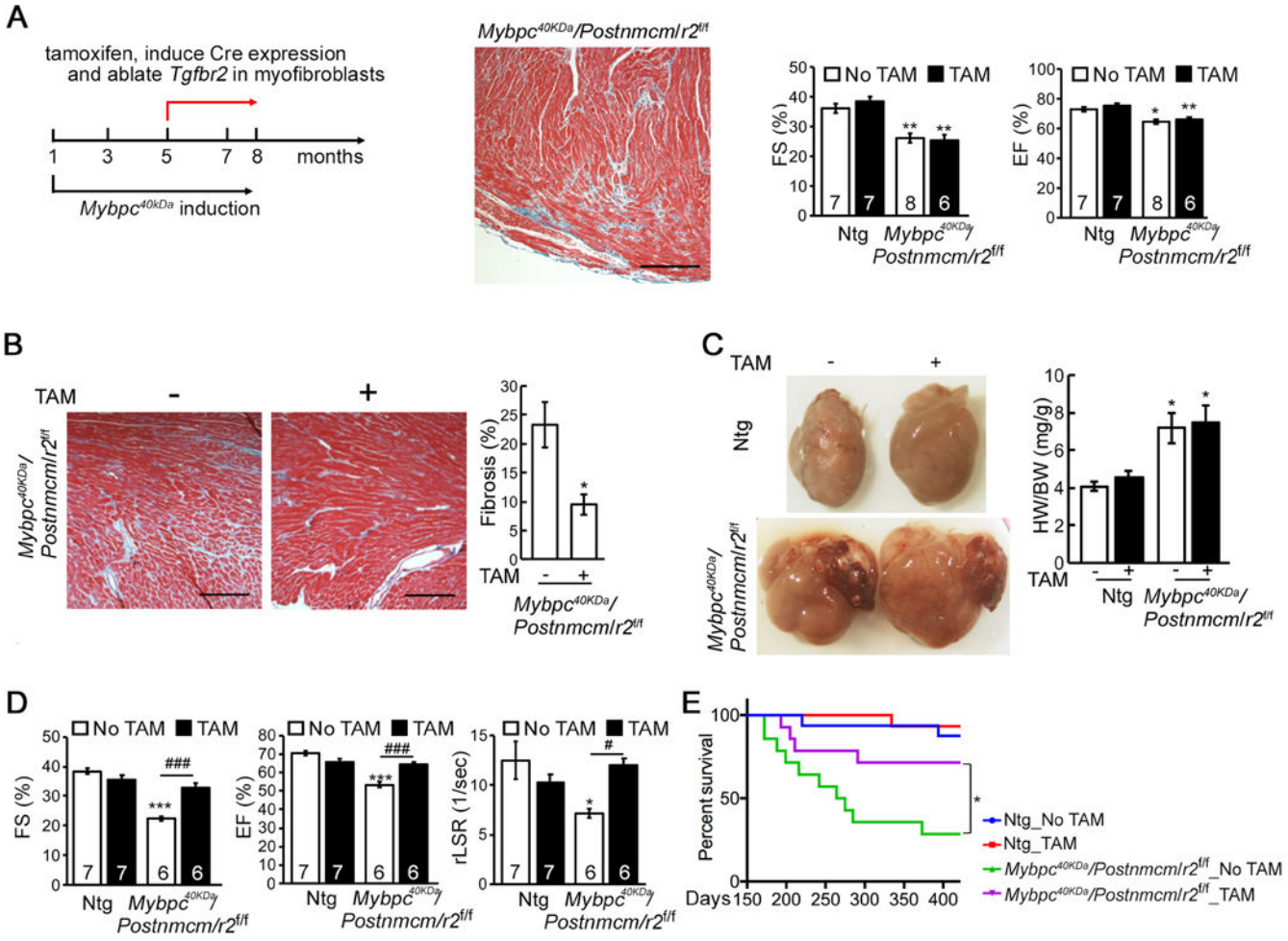

Figure 8.

Late stage myofibroblast specific ablation of Tgfbr2 (r2). **A**, Schematic diagram of the experiment, the degree of fibrosis in the left ventricle, fractional shortening (FS) and ejection fractions (EF) at the time of initiating TAM feeding (5 months of age). Nontransgenic (Ntg) and homozygote ($r2^{f/f}$) nulls of TβRII crossed into the $Mybpc3^{40kDa}$-expressing background. One-way ANOVA analysis with Tukey's post hoc test, *P<0.05, **P<0.01, comparing to Ntg, no TAM group. **B**, Representative Masson's trichrome staining and quantitation of $Mybpc^{40kDa}/Postnmcm/r2^{f/f}$ hearts after 3 months on the TAM (+) or regular (−) chow. Scale bar: 10X, 500 μm. *P<0.05, between group comparison, n=3. **C,** Hearts after 3 months on the TAM (+) or regular (−) chow. The degree of hypertrophy was measured using heart weight/body weight (HW/BW) ratios. One-way ANOVA analysis with Tukey's post hoc test, *P<0.05, compared to Ntg, no TAM group, n=4 for the Ntg group, n=6 for the other groups. **D,** Echocardiographic analyses of the experimental groups. One-way ANOVA analysis with Tukey's post hoc test, ***P<0.001, comparing to Ntg, no TAM group; $^{\#}P$<0.05, $^{\#\#\#}P$<0.001, between group comparison. **E**, Kaplan-Meier survival curve. P<0.0001 using the Log-rank test, n=14–16; all between group comparisons were performed

using the Holm-Šídák post hoc test, *P<0.05. FS; fractional shortening, EF; ejection fraction, rLSR; reverse peak longitudinal strain rate.